*OG.2.2.17*

# Observations of the supernova remnants Cas-A and Tycho with the HEGRA stereoscopic IACT system

**G. Pühlhofer[1], H. Völk[1], C.A. Wiedner[1], for the HEGRA Collaboration**
[1]*Max-Planck-Institut für Kernphysik, Saupfercheckweg 1, D-69117 Heidelberg*

**Abstract**

Recently, young supernova remnants (SNR) from type Ia Supernovae (SNe) have become targets of interest for TeV gamma-ray astronomy. This prompted the HEGRA collaboration to extensively observe Tycho's SNR in 1997 and 1998 with its stereoscopic IACT system. The HEGRA IACT system was also used to observe the young SNR Cas-A. Although considered to be the result of a SN type Ib, the detected strong nonthermal X-ray emission makes this SNR a promising candidate for TeV gamma-ray emission. Given the $0.1^\circ$ spatial resolution of the system, both sources are still nearly pointlike. Therefore, the data samples yield an emission sensitivity close to a few percent of the Crab flux. The Cas-A observations reveal evidence for a TeV signal.

## 1 Introduction

Tycho's SNR is currently considered to be one of the best 'laboratories' to see Cosmic Ray acceleration in Supernova shock waves by the detection of nucleonic induced TeV gamma-rays (Völk, 1997). It is a shell-type remnant of a SN explosion of type Ia which took place in 1572, and is supposed to be currently approaching the end of the sweep-up phase. The shock wave is expanding into a uniform environment with a density of about $1\ \mathrm{cm}^{-3}$. There are no known clouds close to the source. This density implies a rather moderate $\pi^0$-decay flux, the uniformity ensures a rather time-constant flux. Since the dominance of emission lines in the X-ray spectrum is interpreted as evidence that the nonthermal electron component is small, one can be rather confident that eventually detected TeV gamma-rays are of nucleonic origin, and not 'contaminated' with Inverse Compton (IC) gamma-rays. The predicted TeV flux level is $8 \times 10^{-13}\mathrm{cm}^{-2}\mathrm{s}^{-1}$ above 500 GeV, which is below the existing upper limits of the Whipple experiment (Buckley et al., 1998).

The observations of Cas-A were triggered by recent observations of its hard X-ray continuum. Cas-A is assumed to be the remnant of a SN of type Ib, but not driven by a pulsar. The X-ray observations were interpreted as non-thermal synchrotron emission from VHE electrons with energies up to 100 TeV (Allen et al., 1997). This implies an IC gamma-ray flux. Assuming diffusive shock acceleration as the dominant acceleration mechanism, we also expect nucleons of the same energies, and the high ambient matter density favors a strong $\pi^0$-decay flux. However, due to the complex ambient matter configuration, the interpretation of a TeV detection in terms of hadronic vs. leptonic emission would be difficult.

Tycho's SNR and Cas-A are both nearly pointlike in TeV gamma-ray observations ($0.08^\circ$ and $0.05^\circ$ in radius, respectively). Nevertheless, given the excellent angular resolution of $0.09^\circ$ per event of the stereoscopic HEGRA Imaging Atmospheric Cherenkov Telescope (IACT) system, the detection sensitivity for these SNRs is worse than the corresponding excellent point source sensitivity of the present system configuration, which is better than $0.1\mathrm{Crab} \times (\mathrm{t}/25\ \mathrm{h})^{-1/2}$.

## 2 Observational Data

Tycho's SNR and Cas-A were extensively observed with the HEGRA IACT stereoscopic system during summer 1997 and summer 1998 (for a short detector description see Aharonian et al., 1999b, OG.2.1.16). The data were taken with 3 different system configurations: in 1997 with a 4-telescope system (CT3-6); later in 1997 with a 3-telescope system (CT3,5,6); and in 1998 with a 4-telescope system (CT3-6), having a slightly increased energy threshold (+15%) plus most of the time an increased detector dead time, which resulted in a decreased system trigger rate. For a detailed description of the detector performance see e.g. Aharonian et al., 1999a. A further data set, taken with the full system (CT 2-6) on Tycho's SNR in the end of 1998, is not yet

included in this analysis. Mean trigger rates, observation times after run quality selection, and zenith angles are summarized in Table 1.

Table 1: Summary of the data of Tycho's SNR and Cas-A taken with the HEGRA IACT system.

| | system trigger [Hz] | Tycho's SNR | | Cas-A | |
|---|---|---|---|---|---|
| Configuration: | | time [hrs] | mean zenith angle | time [hrs] | mean zenith angle |
| 1: 1997 CT 3-6 | 13 | 20.8 | $37^\circ$ | 49.3 | $31^\circ$ |
| 2: 1997 CT 3,5,6 | 11 | - | | 20.0 | $32^\circ$ |
| 3: 1998 CT 3-6 | 11.5 | 16.8 | $36^\circ$ | 58.6 | $33^\circ$ |
| Total | | 37.6 | | 127.9 | |

All data were taken using the IACT system standard mode for point source observations, the so called wobble mode. Here run pairs of 20 to 30 min each are taken with the source alternatingly displaced from the center of the field of view by $\pm 0.5^\circ$ in declination. Since the IACT system has a field of view (FOV) of $2^\circ$ diameter with a homogeneous acceptance for gamma and cosmic rays (CR), the expected CR background in the source region can be determined with high statistical accuracy from off-source regions in the FOV; this is not noticeably affected by the slightly extended source images of the two SNRs.

# 3 Analysis Methods

For each individual shower, induced by a TeV gamma or CR, the stereoscopic reconstruction is used to determine the particle origin in celestial coordinates and the projected particle impact point on the ground (also called shower core). For primary gamma rays, the angular accuracy is $0.09^\circ$ per event, with a systematic pointing accuracy of better than $0.01^\circ$ (Pühlhofer et al., 1997).

In order to reduce the CR induced background, the shower image shapes as measured under different viewing angles with different telescopes, are compared to expected values, taking into account the measured image amplitudes, the distance of the telescopes to the measured shower core, and the zenith angle. The standard image cut parameter used in the IACT system observations is the so called *mean scaled width* parameter $< \tilde{w} >$ (Aharonian et al., 1999a). This cut was found to be very robust. A cut of $< \tilde{w} >< 1.1$ provides optimum signal to noise enhancement. In order to reduce the background further, more image parameters and the fluctuations in CR induced showers can be taken into account, using e.g. the probability cut introduced in Daum et al., 1997. Here a probability $\mathrm{p}_\gamma$ is calculated for the assumption of a gamma ray induced shower, as in equation (1),

$$\mathrm{p}_\gamma = \prod_{tel} \rho_w^\gamma(\mathrm{width}_{tel} \mid \mathrm{amp}_{tel}, \mathrm{dtc}_{tel}, \mathrm{zen})\ \rho_l^\gamma(\mathrm{width}_{tel} \mid \mathrm{amp}_{tel}, \mathrm{dtc}_{tel}, \mathrm{zen}) \quad (1)$$

and similarly for the assumption of a CR induced shower. $\rho_w^\gamma$ is the probability that the measured width is due to a primary gamma ray, and so on. $\mathrm{p}_\gamma$ must exceed $\mathrm{p}_{CR}$ by a certain value. This cut further reduces the background, but is currently found to be not as stable regarding the gamma ray efficiency $\kappa_\gamma$, compared to the mean scaled width cut. The probability cut is presently only used in the search for faint sources, but needs further studies before it can be used to determine flux limits.

In Table 2 the efficiencies of both cuts at zenith angles $30^\circ - 40^\circ$ are shown where the SNR observations were made. For determination of the gamma ray efficiency data from Mrk501 in a high flux state in 1997 (Aharonian et al., 1999b, OG.2.1.16) was used.

The signal region used has a radius of $0.17^\circ$. This is slightly larger than the optimum angular cut applied for the search for point sources, in order to account for the slightly extended source images. Background estimates come from control regions in the FOV, either from a circle at the opposite side of the FOV, or from a ring segment around the source location; both are in good agreement, and their statistical errors are small.

Table 2: Gamma ray and CR efficiencies of the image shape cuts applied in this analysis.

| | $< \tilde{w} >< 1.1$ | | $p_\gamma$compared to $p_{CR}$ | |
|---|---|---|---|---|
| | $\kappa_\gamma$ from ON-OFF | $\kappa_{CR}$ from OFF | $\kappa_\gamma$ from ON-OFF | $\kappa_{CR}$ from OFF |
| Mrk-501 | $0.73 \pm 0.06$ | 0.068 | $0.50 \pm 0.04$ | 0.025 |
| Tycho's SNR | - | 0.068 | - | 0.023 |
| Cas-A | - | 0.066 | - | 0.024 |

# 4 Results

Table 3 shows the measured excess counts and their statistical significance.

Table 3: Excess counts after image and angular cuts.

| | configuration | shape cut | excess counts | expected background | excess significance above background in standard deviations |
|---|---|---|---|---|---|
| Tychos's SNR | 1 | $< \tilde{w} >< 1.1$ | 36.3 | $323.7 \pm 6.1$ | 1.9 |
| | | prob. cut | -5.7 | $111.7 \pm 3.5$ | -0.5 |
| | 3 | $< \tilde{w} >< 1.1$ | -13.9 | $200.9 \pm 4.8$ | -0.9 |
| | | prob. cut | -10.0 | $68.0 \pm 2.8$ | -1.1 |
| Cas-A | 1 | $< \tilde{w} >< 1.1$ | 33.8 | $772.2 \pm 9.4$ | 1.2 |
| | | prob. cut | 44.1 | $275.9 \pm 5.6$ | 2.5 |
| | 2 | $< \tilde{w} >< 1.1$ | 29.7 | $270.3 \pm 5.6$ | 1.7 |
| | | prob. cut | -1.7 | $96.7 \pm 3.2$ | -0.2 |
| | 3 | $< \tilde{w} >< 1.1$ | 149.3 | $668.7 \pm 8.8$ | 5.4 |
| | | prob. cut | 74.3 | $231.7 \pm 5.2$ | 4.6 |

Table 4: Combined significances in units of standard deviations.

| | significance above background | |
|---|---|---|
| | $< \tilde{w} >< 1.1$ | prob. cut |
| Cas-A | 4.9 | 4.5 |
| Tycho's SNR | 0.9 | -1.1 |

In Figure 1 the so called $\theta^2$-plots of Cas-A in 1997, configuration 1, and 1998, configuration 3, after probability cuts are shown. Here the counts vs. the distance squared to the source position are plotted; in this representation the expected background produces a flat distribution, the signal region is centered around 0.

Table 4 gives the combined significances, ignoring so far the slightly different sensitivities of the three configurations. So far no signal in the Tycho's SNR observation can be seen, but a larger part of data still has to be included in this analysis. The Cas-A observations reveal evidence for a TeV-signal. At the current status of the analysis, results are still preliminarily. Further investigations on detector and cut efficiencies are under way, and will be presented at the conference.

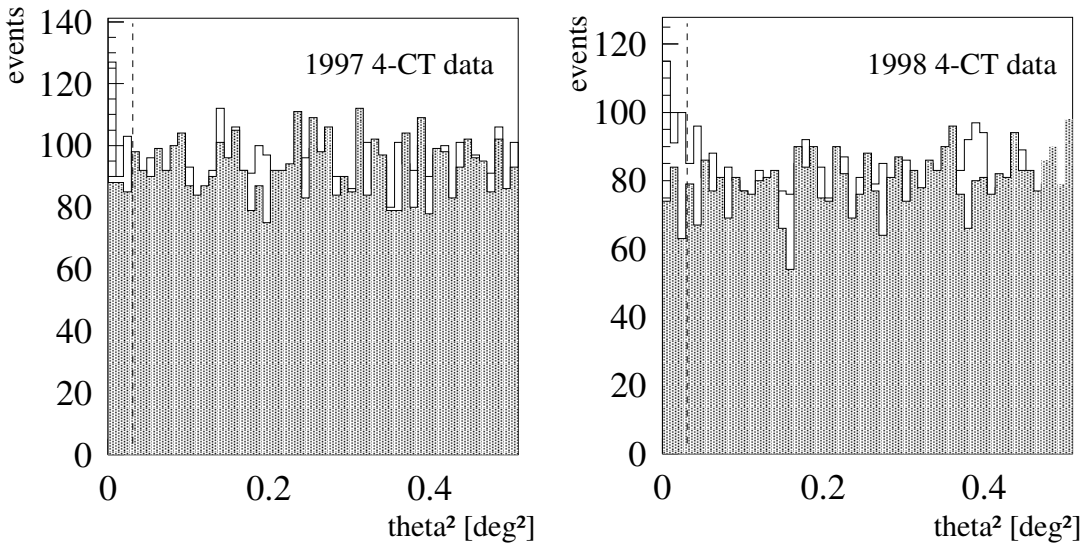


Figure 1: $\theta^2$-plot of the Cas-A observations of configuration 1 (left) and configuration 3 (right). The optimum angular cut for the given source extentions is indicated by the vertical dashed lines. The shaded histogram shows the background.

# References

Allen et al., 1997, ApJ 487, L97
Aharonian, F., et al. 1999a, A&A 342, 69
Aharonian, F., et al. 1999b, Proc. 26th ICRC (Salt Lake City), OG.2.1.16
Buckley et al., 1998, A&A 329, 639
Daum, A., et al. 1997, Astrop. Phys. 8, 1.
Pühlhofer, G. et al. 1997, Astrop. Phys. 8, 101
Völk, H.J. 1997, Proc. "Towards a Major Atmospheric Cherenkov Detector II", (South Africa)